清華大學
Tsinghua University

Boltzmann transport equation (BTE)-based multiscale modeling of electron hydrodynamics

Yunfan Huang
Department of Engineering Mechanics
Tsinghua University
2024.06.13

Contents

- Introduction to viscous electron transport
- Multiscale modeling and various possibilities
- Case study: Magnetoresistance in hydrodynamic regime
  - Mesoscopic eBTE formulation
  - Verification of numerical methods (DOM)
  - Evaluation of macroscopic description
  - Results of magnetoresistance simulation
- Conclusions

Contents

- Introduction to viscous electron transport
- Multiscale modeling and various possibilities
- Case study: Magnetoresistance in hydrodynamic regime
  - Mesoscopic eBTE formulation
  - Verification of numerical methods (DOM)
  - Evaluation of macroscopic description
  - Results of magnetoresistance simulation
- Conclusions

There's plenty of room at the bottom: energy-ZT$_e$

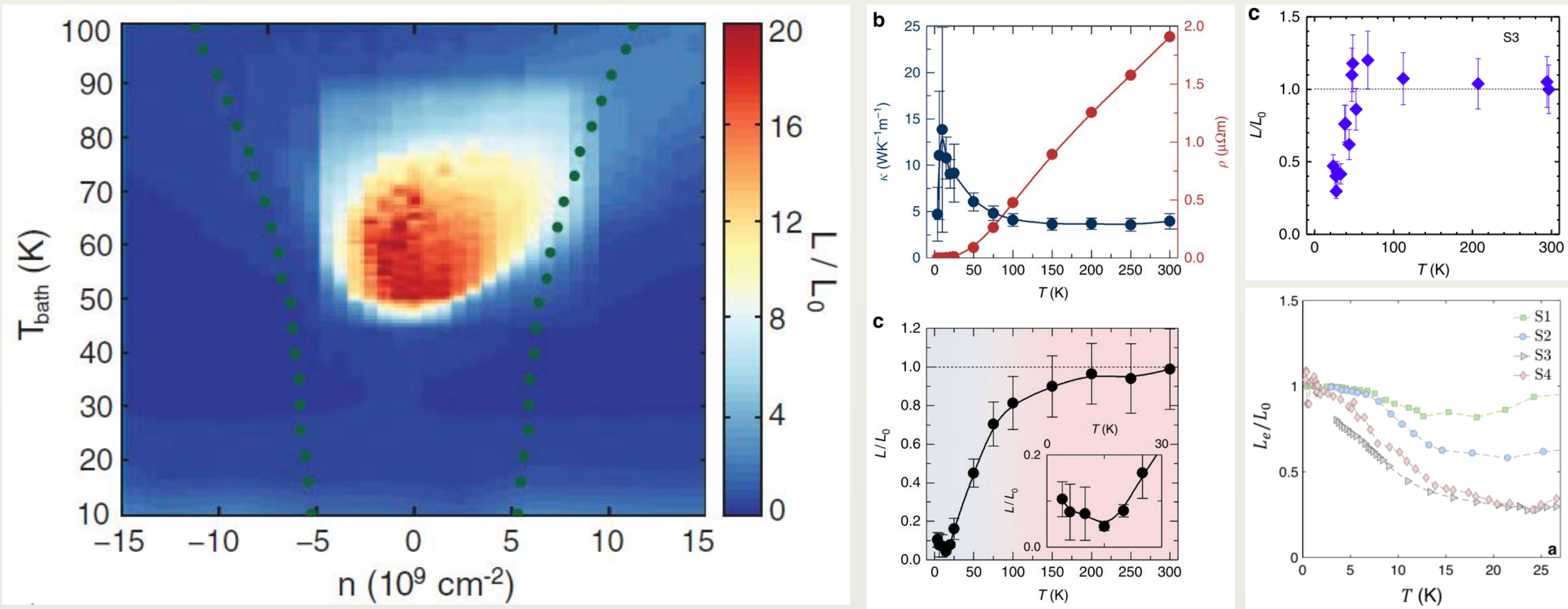

Breakdown of W-F law in graphene (left) & WP_2 (mid) & MoP (r-top) & Sb (r-bot)

$$\mathrm{ZT} = S^2/\mathcal{L} \quad \mathcal{L} \equiv \frac{\kappa_e}{\sigma T} = \frac{\pi^2}{3}\left(\frac{k_B}{e}\right)^2 \equiv \mathcal{L}_0$$

higher/lower κ_e than W-F law

- ✓ **System: 2D material, ultrapure, low T**
- ✓ **Phenomena: Anomalous transport of 2D electrons**
- ✓ **Impact: low heat loss in thermoelectric materials**

Crossno J. et al. *Science*. 2016, **351**: 1058-1061.
Gooth, J., et al., *Nature Communications*, 2018. **9**(1): 4093; Jaoui, A., et al., *npj Quantum Materials*, 2018. **3**(1): 64.
Kumar, N., et al., *Nature Communications*, 2019. **10**(1): 2475.
Jaoui, A., B. Fauqué, and K. Behnia, *Nature Communications*, 2021. **12**(1): 195.

There's plenty of room at the bottom: info-σ_e

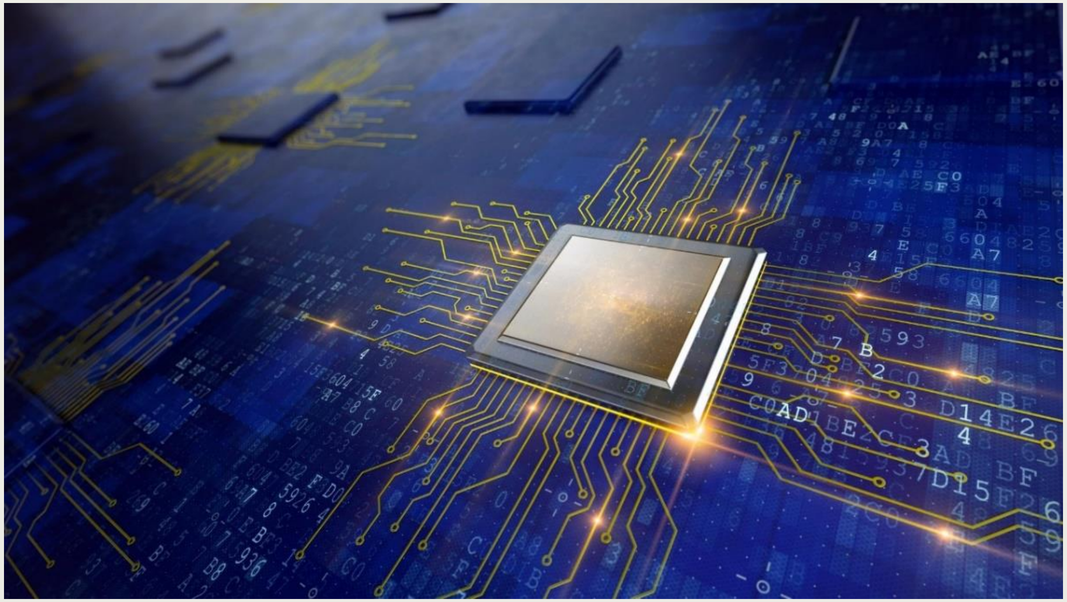

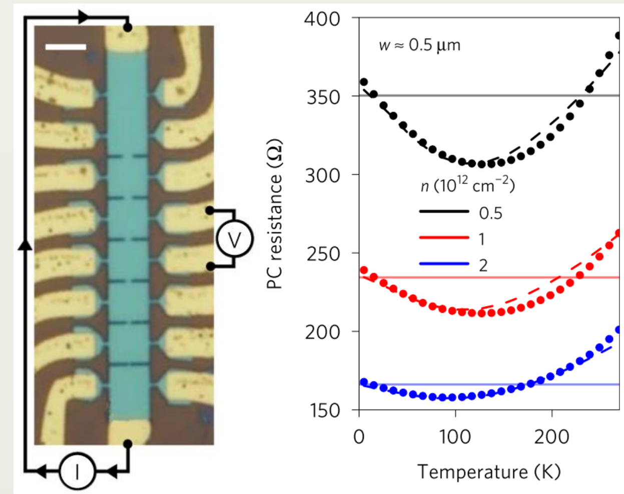

Super-ballistic flow in confined graphene

$$\boldsymbol{j} = \sigma \boldsymbol{E}$$

High electron conductivity

Low heat generation → **High** current transport capability

High cutoff frequency → **Low** switching time of the transistor

- **System: 2D materials, ultra-pure, microscale and low-T**
- **Phenomena: high mobility, may improve performance of semiconductors**

[1] Kumar K.R. et al. *Nature Physics*, 2017, **13**(12): 1182-5

There's plenty of room at the bottom: physics-j_e

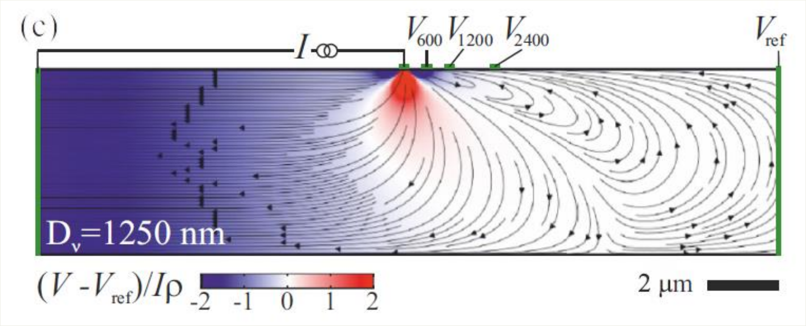

Electron **backflow** in GaAs/GaAlAs

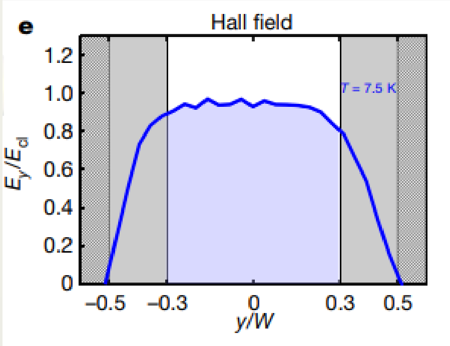

Ballistic regime

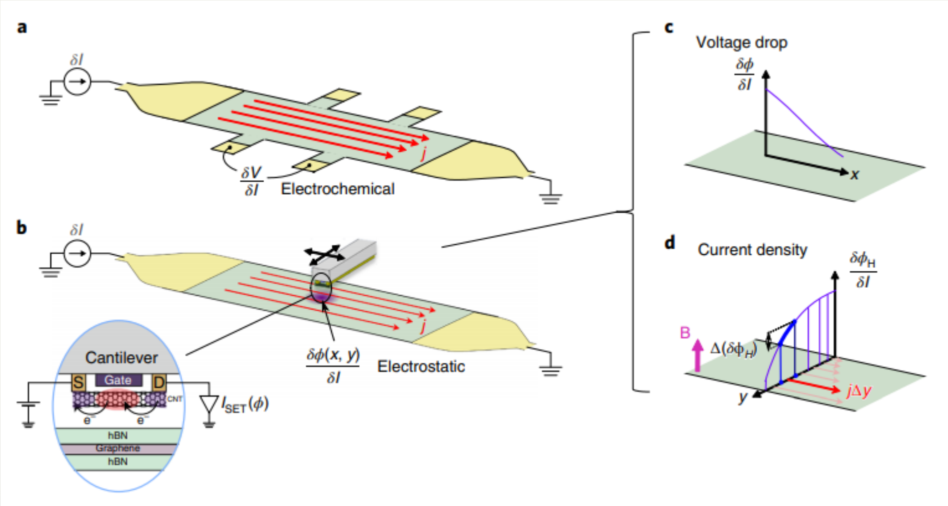

Conventional (a) and SET-based (b) measurement for current profile

$$E_y \sim j_x(+\partial_y^2 j_x)$$

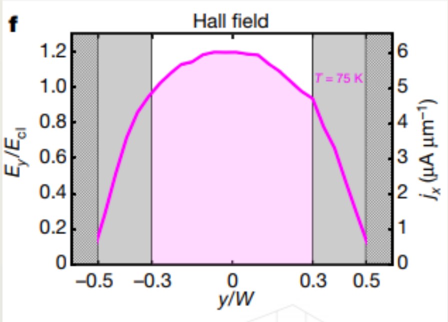

Viscous regime

- ✓ **System: Low-D, low-T**
- ✓ **Phenomena: Emergence of viscosity?**

[1] Braem B.A. et al. *Phys. Rev. B*, 2018, **98**: 241304
[2] Ella, L., et al. *Nature Nanotechnology*, 2019.
[3] Sulpizio, J. A., et al. *Nature*, 2019.

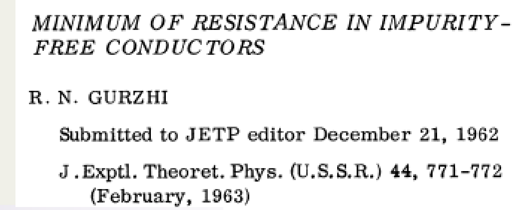
MINIMUM OF RESISTANCE IN IMPURITY-FREE CONDUCTORS

R. N. GURZHI

Submitted to JETP editor December 21, 1962

J.Exptl. Theoret. Phys. (U.S.S.R.) 44, 771-772 (February, 1963)

The first paper

Electric resistance in 2D electron transport

Bulk material

- Room T: Phonon scattering dominates
- Low T: Defect scattering dominates

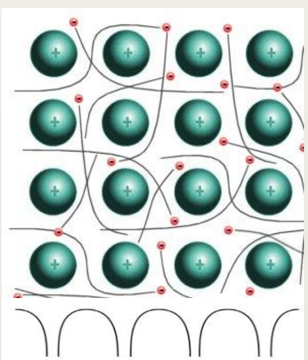

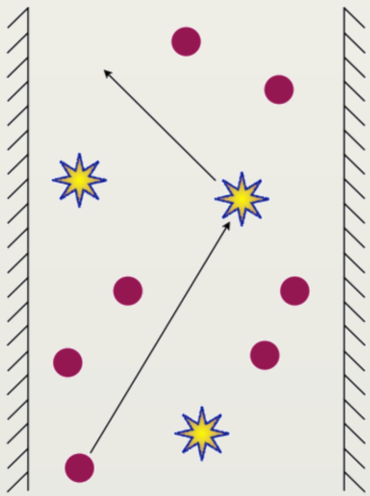

Nearly Free electron model

Electron ⟷ Lattice*

Lattice-induced resistance

* Refers to phonons and defects.

Confined material

Low T: Phonon scattering becomes weak
Ultra-pure: Defect scattering becomes weak

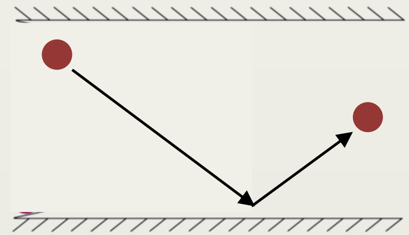

Nearly Free electron model

Electron ⟷ Boundary

Viscous electron fluid

Electron ⟷ Electron

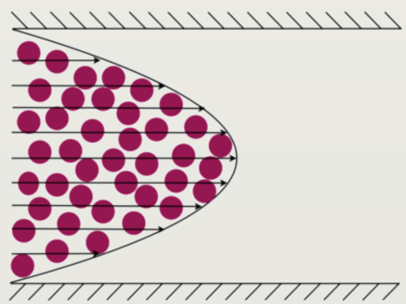

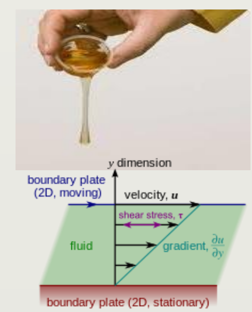

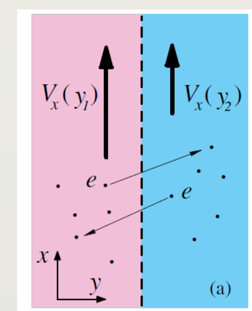

Boundary-induced resistance + Bulk viscosity

→ Electron magneto-hydrodynamics

[1] Polini M, Geim A K. Viscous electron fluids. *arXiv*, 2019.

Review/perspectives on eHD in metal [1]

1. Gurzhi, R.N., Hydrodynamic effects in solids at low temperature. *Sov. Phys. Usp.*, 1968. **11**: 255.
2. Gurzhi, R.N. and A.I. Kopeliovich, Low-temperature electrical conductivity of pure metals. *Sov. Phys. Usp.*, 1981. **24**(1): 17.
3. Kaveh, M. and N. Wiser, Electron-electron scattering in conducting materials. *Advances in Physics*, 1984. **33**(4): 257-372.
4. Wiser, N., The electrical resistivity of the simple metals. *Contemporary Physics*, 1984. **25**(3): 211-249.
5. Lee, P.A. and T.V. Ramakrishnan, Disordered electronic systems. *Reviews of Modern Physics*, 1985. **57**(2): 287-337.
6. van Vucht, R.J.M., H. van Kempen, and P. Wyder, Simple transport properties of simple metals: classical theories and modern experiments. *Reports on Progress in Physics*, 1985. **48**(6): 853–905.
7. Bass, J., W.P. Pratt, and P.A. Schroeder, The temperature-dependent electrical resistivities of the alkali metals. *Rev. Mod. Phys.*, 1990. **62**: 645–744.
8. Gasparov, V.A. and R. Huguenin, Electron-phonon, electron-electron and electron-surface scattering in metals from ballistic effects. *Advances in Physics*, 1993. **42**(4): 393-521.

Review/perspectives on eHD in 2D materials [2]

9. Zaanen, J., Electrons go with the flow in exotic material systems. *Science,* 2016. **351**(6277): 1026–1027.
10. Narozhny, B.N., *et al.,* Hydrodynamic Approach to Electronic Transport in Graphene. *Annalen der Physik*, 2017. **529**(11): 1700043.
11. Lucas, A. and K.C. Fong, Hydrodynamics of electrons in graphene. *Journal of Physics: Condensed Matter*, 2018. **30**(5): 053001.
12. Lucas, A., An exotic quantum fluid in graphene. *Science*, 2019. **364**(6436): 125.
13. Narozhny, B.N., Electronic hydrodynamics in graphene. *Annals of Physics*, 2019. **411**: 167979.
14. Polini, M. and A.K. Geim, Viscous electron fluids. *Physics Today*, 2020.
15. Matthaiakakis, I., Hydrodynamics in Solid State Systems and the AdS/CFT correspondence. 2021.
16. Narozhny, B.N., Hydrodynamic approach to two-dimensional electron systems. *La Rivista del Nuovo Cimento*, 2022.

Review/perspectives on eHD-related 2D materials [3]

17. Stern, F. and W.E. Howard, Properties of Semiconductor Surface Inversion Layers in the Electric Quantum Limit. *Physical Review*, 1967. **163**(3): p816-835.
18. Beenakker, C.W.J. and H. van Houten, Quantum Transport in Semiconductor Nanostructures. *Solid State Physics*, 1991. **44**: 1-228.
19. Castro Neto, A.H., et al., The electronic properties of graphene*. Rev. Mod. Phys.,* 2009. **81**: 109–162.
20. Kotov, V.N., et al., Electron-Electron Interactions in Graphene: Current Status and Perspectives. *Rev. Mod. Phys.*, 2012. **84**: 1067–1125.
21. Novoselov, K.S., et al., A roadmap for graphene. *Nature*, 2012. **490**(7419): 192-200.
22. Kushwaha, P., et al., Nearly free electrons in a 5d delafossite oxide metal. *Science Advances*, 2015. **1**(9): e1500692.
23. Mackenzie, A.P., The properties of ultrapure delafossite metals. *Reports on Progress in Physics*, 2017. **80**(3): 032501.
24. Wu, J., et al., Perspectives on Thermoelectricity in Layered and 2D Materials. *Advanced Electronic Materials*, 2018. **4**(12): p1800248.

Contents

- Introduction to viscous electron transport
- Multiscale modeling and various possibilities
- Case study: Magnetoresistance in hydrodynamic regime
  - Mesoscopic eBTE formulation
  - Verification of numerical methods (DOM)
  - Evaluation of macroscopic description
  - Results of magnetoresistance simulation
- Conclusions

From phenomenological to multiscale modeling

- **Macroscopic model: Electron N-S equation**

$$\frac{\partial \boldsymbol{v}}{\partial t} = \eta_{xx}\Delta\boldsymbol{v} + \eta_{xy}\Delta\boldsymbol{v}\times\boldsymbol{e}_z + \frac{e}{m}(-\nabla\varphi + \boldsymbol{v}\times\boldsymbol{B}) - \frac{\boldsymbol{v}}{\tau}$$

$$\left[\boldsymbol{v}_t + \frac{\boldsymbol{\sigma}_{nt}}{\rho\nu} l_b\right]_\Sigma = 0$$

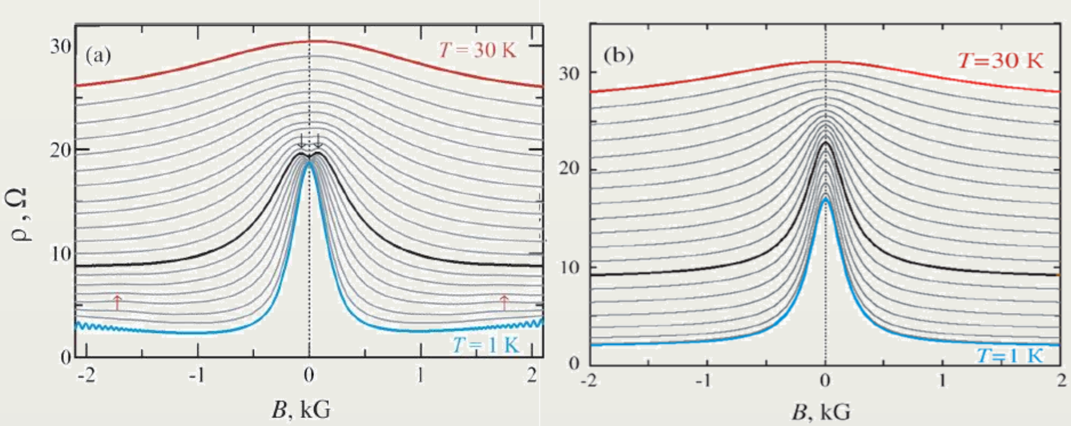

Experiment　　Theory

$$\rho \sim \frac{1}{\tau} + \frac{1}{\tau^\star}\frac{1}{1+(2\omega_c\tau_2)^2}$$

$$\begin{cases} \omega_c \sim B \\ \tau \sim \tau_{\mathrm{ep}} \\ \tau^\star \sim w^2/\tau_{\mathrm{ee}} \\ \tau_2 \sim \tau_{\mathrm{ee}} \end{cases}$$

- **Strengths**
  - simple & direct to include collective effect, inspiring for physical modelling
  - able to solve complex problems with relatively low computational cost
- **Weaknesses**
  - insufficient to study the microscopic mechanism
  - unclear about the applicability of the phenomenological theories

[1] Gurzhi R N. *Sov. Phys. JETP.*, 1963, **17**: 521.
[2] Gurzhi R P, Shevchenko S I. *Sov. Phys. JETP.*, 1968, **27**: 1019.
[3] Alekseev P S, Semina M A. *Phys. Rev. B*, 2018, **98**: 165412.

From phenomenological to multiscale modeling

- **Microscopic model: Electron drift-diffusion equation**

$$m\frac{\mathrm{d}\boldsymbol{V}}{\mathrm{d}t}+\gamma\boldsymbol{V}=\boldsymbol{F}(t)+\boldsymbol{R}(t)$$

- Basis of test-particle method, an example of Monte Carlo method
- Collision term based on BTE, which has been utilized in transport of neutron/photon/electron/phonon

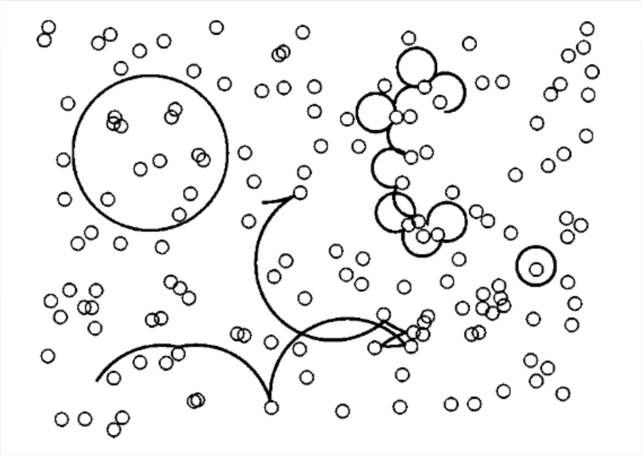

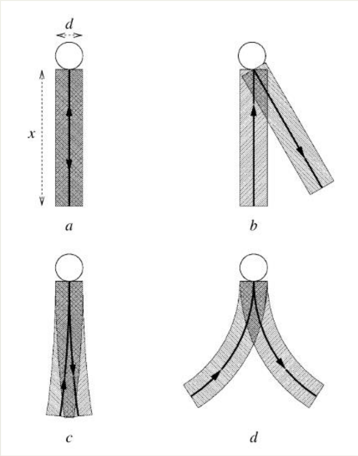

- **Strengths**
  - simple & direct to include resistance scattering and geometric barriers
  - easy to consider the collective effect based on scattering models in BTE
- **Weaknesses**
  - relatively high computational cost for complex problems
  - less physical intuitive for the phenomenological hydrodynamic mechanism

[1] Dmitriev, A., M. Dyakonov, and R. Jullien, *Physical Review B*, 2001, **64**(23): 233321
[2] Dmitriev, A., M. Dyakonov, and R. Jullien, *Physical Review Letters*, 2002, **89**(26): 266804.

From phenomenological to multiscale modeling

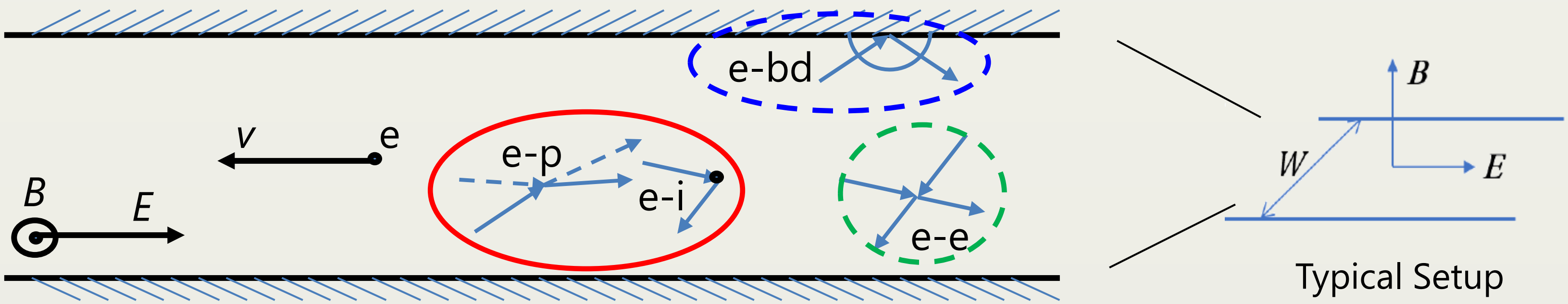

- Resistive scattering $\boldsymbol{p}_{\text{out}} \neq \boldsymbol{p}_{\text{in}}$
- Conservative scattering $\boldsymbol{p}_{\text{out}} = \boldsymbol{p}_{\text{in}}$

  } Body scattering
- Boundary scattering $\boldsymbol{p}_{\text{out}} = \text{aver}\left(\boldsymbol{p}_{\text{reflection}}, \boldsymbol{p}_{\text{random}}\right)$

- **Boltzmann transport equation (BTE)**

$$\boxed{\frac{\mathrm{d}f}{\mathrm{d}t}} = \frac{\partial f}{\partial t} + \boldsymbol{v} \cdot \frac{\partial f}{\partial \boldsymbol{r}} + \frac{\boldsymbol{F}}{m} \cdot \frac{\partial f}{\partial \boldsymbol{v}} = \boxed{C(f)} \begin{cases} \text{Resistive} & l_{\text{MR}} & f_0(\boldsymbol{r}, \varepsilon_{\boldsymbol{k}}) \\ \text{Conservative} & l_{\text{MC}} & f_0(\boldsymbol{r}, \varepsilon_{\boldsymbol{k}} - \boldsymbol{u} \cdot \boldsymbol{p}) \end{cases}$$

zero local velocity

collective moving velocity

Change of electron state ⇐ **Electron scattering** | **Different mechanisms** ⇒ **Different (quasi-) equilibrium states**

[1] De Jong M J M, Molenkamp L W. Phys. Rev. B, 1995, **51**: 13389-13402.
[2] Scaffidi, T., et al., *Physical Review Letters*, 2017, **118**(22): 226601.

Plenty of possibilities of electron hydrodynamics

Multiscale feature:

Mesoscopic BTE

Numerical Algorithm

Up-scaling method

Discrete ordinate method (MESO)

Electron hydrodynamic equation (MACRO)

Numerical solution

Theoretical solution

verification

Interdisciplinary feature:

ElectronHD v.s. classical electron transport

- Conductivity (T-dependence)
- Vortices in flow fields (viscosity)
- Boundary layers ("electron-kinetics")
- Pre-turbulence (instability)
- Shock | shadow wave (non-linear)

ElectronHD v.s. classical hydrodynamics

- Relaxation effect (resistance)
- Magneto-resistance (multi-physical)
- Hall viscosity effect (odd viscosity)
- Non-equilibrium effect (ballistic)
- Non-local effect (correlation)

Reports on eHD based on direct imaging [1]

1. Braem, B.A., et al., Scanning gate microscopy in a viscous electron fluid. *Physical Review B*, 2018. **98**(24): 241304.
2. Ella, L., et al., Simultaneous voltage and current density imaging of flowing electrons in two dimensions. *Nature Nanotechnology*, 2019. **14**(5): 480-487.
3. Sulpizio, J.A., et al., Visualizing Poiseuille flow of hydrodynamic electrons. *Nature*, 2019. **576**(7785): 75-79.
4. Jenkins, A., et al., Imaging the breakdown of ohmic transport in graphene. arXiv: 2002.05065v3, 2020.
5. Ku, M.J.H., et al., Imaging viscous flow of the Dirac fluid in graphene. *Nature*, 2020. **583**(7817): 537-541.
6. Aharon-Steinberg, A., et al., Direct observation of vortices in an electron fluid. *Nature*, 2022. **607**(7917): 74-80.
7. Kumar, C., et al., Imaging hydrodynamic electrons flowing without Landauer–Sharvin resistance. *Nature*, 2022. **609**(7926): 276-281.
8. Krebs, Z.J., et al., Imaging the breaking of electrostatic dams in graphene for ballistic and viscous fluids. *Science*, 2023. **379**(6633): 671-676.

Reports on eHD based on indirect measuring (E) [2]

1. Bandurin, D.A., et al., Negative local resistance caused by viscous electron backflow in graphene. *Science*, 2016. **351**(6277): 1055.
2. Lee, M., et al., Ballistic miniband conduction in a graphene superlattice. *Science*, 2016. **353**(6307): 1526-1529.
3. Levitov, L. and G. Falkovich, Electron viscosity, current vortices and negative nonlocal resistance in graphene. *Nature Physics*, 2016. **12**: 672-672.
4. Guo, H., et al., Higher-than-ballistic conduction of viscous electron flows. *Proceedings of the National Academy of Sciences*, 2017. **114**(12): 3068–3073.
5. Krishna Kumar, R., et al., Superballistic flow of viscous electron fluid through graphene constrictions. *Nature Physics*, 2017. **13**(12): 1182-1185.
6. Bandurin, D.A., et al., Fluidity onset in graphene. *Nature Communications*, 2018. **9**(1): 4533-4533.
7. Komatsu, K., et al., Observation of the quantum valley Hall state in ballistic graphene superlattices. *Science Advances*, 2018. **4**(5): p. eaaq0194.
8. Gallagher, P., et al., Quantum-critical conductivity of the Dirac fluid in graphene. *Science*, 2019. **364**(6436): p. 158–162-158–162.
9. Di Sante, D., et al., Turbulent hydrodynamics in strongly correlated Kagome metals. *Nature Communications*, 2020. **11**: 3997.

Reports on eHD based on indirect measuring (T) [3]

1. Crossno, J., et al., Observation of the Dirac fluid and the breakdown of the Wiedemann-Franz law in graphene. *Science*, 2016. **351**(6277): 1058.
2. Gooth, J., et al., Thermal and electrical signatures of a hydrodynamic electron fluid in tungsten diphosphide. *Nature Communications*, 2018. **9**(1): 4093.
3. Jaoui, A., et al., Departure from the Wiedemann–Franz law in WP2 driven by mismatch in T-square resistivity prefactors. *npj Quantum Materials*, 2018. **3**(1): 64.
4. Kumar, N., et al., Extremely high conductivity observed in the triple point topological metal MoP. *Nature Communications*, 2019. **10**(1): 2475.
5. Jaoui, A., B. Fauqué, and K. Behnia, Thermal resistivity and hydrodynamics of the degenerate electron fluid in antimony. *Nature Communications*, 2021. **12**(1): 195.

Reports on eHD based on indirect measuring (B) [4]

1. Sarginson, K. and D.K.C. Macdonald, Influence of a Magnetic Field on the Size-Variation of Electrical Conductivity. *Nature*, 1949. **164**(4178): 921-922.
2. Sondheimer, E.H., Influence of a Magnetic Field on the Conductivity of Thin Metallic Films. *Nature*, 1949. **164**(4178): 920-921.
3. Lucas, A., R.A. Davison, and S. Sachdev, Hydrodynamic theory of thermoelectric transport and negative magnetoresistance in Weyl semimetals. *Proceedings of the National Academy of Sciences*, 2016. **113**(34): 9463.
4. Moll, P.J.W., et al., Evidence for hydrodynamic electron flow in PdCoO2. *Science*, 2016. **351**(6277): 1061–1064.
5. Berdyugin, A.I., et al., Measuring Hall viscosity of graphene's electron fluid. *Science*, 2019. **364**(6436): 162.

Reports on eHD based on mesoscopic simulation [5]

1. Menne, R. and R.R. Gerhardts, Magnetoresistance of a two-dimensional electron gas with spatially periodic lateral modulations: Exact consequences of Boltzmann's equation. *Physical Review B*, 1998. **57**(3): p. 1707-1722.
2. Dmitriev, A., M. Dyakonov, and R. Jullien, Classical mechanism for negative magnetoresistance in two dimensions. *Physical Review B*, 2001. **64**(23): p. 233321.
3. Dmitriev, A., M. Dyakonov, and R. Jullien, Anomalous Low-Field Classical Magnetoresistance in Two Dimensions. *Physical Review Letters*, 2002. **89**(26): p. 266804.
4. Govorov, A.O. and J.J. Heremans, Hydrodynamic Effects in Interacting Fermi Electron Jets. *Physical Review Letters*, 2004. **92**(2): p. 026803.
5. Yi, C., Hybrid discrete ordinates and characteristics method for solving the linear Boltzmann equation. 2007.
6. Delacrétaz, L.V. and A. Gromov, Transport Signatures of the Hall Viscosity. *Phys. Rev. Lett*., 2017. **119**: p. 226602-226602.
7. Scaffidi, T., et al., Hydrodynamic Electron Flow and Hall Viscosity. *Physical Review Letters*, 2017. **118**(22): p. 226601.
8. Coelho, R.C.V. and M.M. Doria, Lattice Boltzmann method for semiclassical fluids. *Comput. Fluids*, 2018. **165**: p. 144-159.
9. Gabbana, A., et al., Prospects for the Detection of Electronic Preturbulence in Graphene. *Phys. Rev. Lett*., 2018. **121**: p. 236602-236602.
10. Gorbar, E.V., et al., Nonlocal transport in Weyl semimetals in the hydrodynamic regime. *Physical Review B*, 2018. **98**(3): p. 035121.
11. Moessner, R., P. Surówka, and P. Witkowski, Pulsating flow and boundary layers in viscous electronic hydrodynamics. *Phys. Rev. B*, 2018. **97**: p. 161112-161112.
12. Chandra, M., et al., Hydrodynamic and ballistic AC transport in two-dimensional Fermi liquids. *Phys. Rev. B*, 2019. **99**: p. 165409-165409.
13. Danz, S. and B.N. Narozhny, Vorticity of viscous electronic flow in graphene. *2D Materials*, 2020. **7**(3): p. 035001.
14. Varnavides, G., et al., Generalized Electron Hydrodynamics, Vorticity Coupling, and Hall Viscosity in Crystals, in arXiv e-prints. 2020.

Another topic: electrokinetics ([离子]电动理学)

- 电动流体力学的研究对象：电解质溶液中带电界面附近双电层内离子与流体的耦合输运

微观界面作用机理 ⟶ 宏观流动典型现象

带电界面附近存在净电荷区 (双电层)
电化学势梯度诱导流体与壁面产生剪切

界面电荷输运与体相流体流动强烈耦合：
流体电渗流动，颗粒电泳运动，电解质溶液导电…

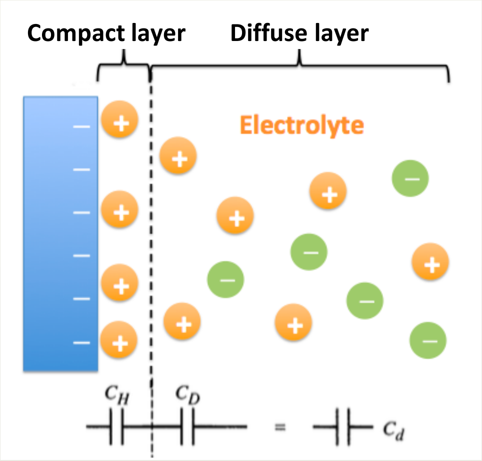

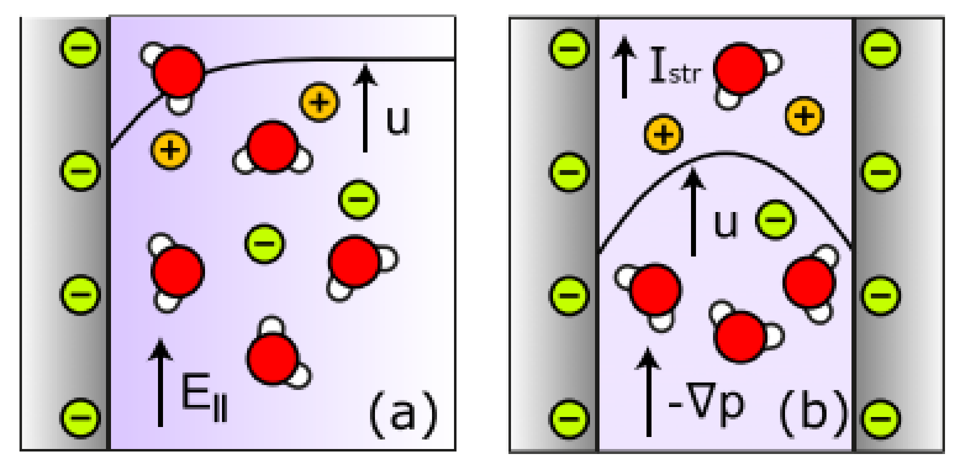

微观双电层厚度 = 1~100 nm

宏观流动尺度 = μm 甚至 mm 量级

界面电动流动的基本特征：多物理（流动与离子输运耦合），跨尺度（界面薄层引起宏观流动）

[1] Onsager, L., Report on a revision of the conductivity theory. *Transactions of the Faraday Society*, 1927. **23**: 341-349.
[2] Onsager, L. and R.M. Fuoss, Irreversible Processes in Electrolytes. Diffusion, Conductance and Viscous Flow in Arbitrary Mixtures of Strong Electrolytes. *The Journal of Physical Chemistry*, 1931. **36**: 2689-2778.
[3] Onsager, L., Reciprocal Relations in Irreversible Processes. *Phys. Rev.*, 1931. **37**(4): 405-426; 1931. **38**: 2265–2279.

Contents

- Introduction to viscous electron transport
- Multiscale modeling and various possibilities
- Case study: Magnetoresistance in hydrodynamic regime
    - Mesoscopic eBTE formulation
    - Verification of numerical methods (DOM)
    - Evaluation of macroscopic description
    - Results of magnetoresistance simulation
- Conclusions

Mesoscopic method based on electron BTE

$$\frac{\partial f}{\partial t}+\boldsymbol{v}\cdot\frac{\partial f}{\partial \boldsymbol{r}}+\frac{\boldsymbol{F}}{m}\cdot\frac{\partial f}{\partial \boldsymbol{v}}=C(f)=:-\frac{f-P_0[f]}{\tau_{\mathrm{MR}}}-\frac{f-P[f]}{\tau_{\mathrm{MC}}}$$

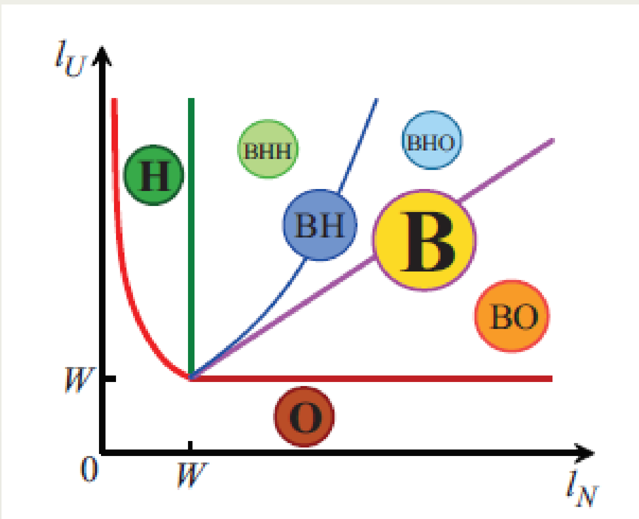

Phase diagram of transport
by **theoretical evaluation**

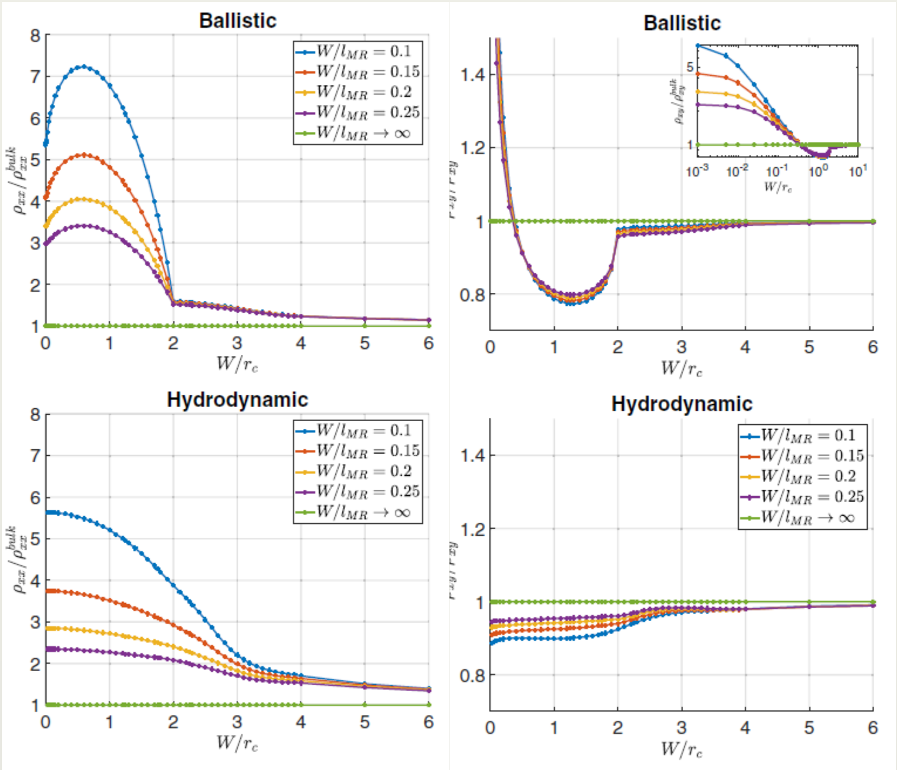

Magneto-resistance effect
by **numerical simulation**

[1] Alekseev P.S. and Semina M.A. *Phys. Rev. Lett*, 2018, **98**: 165412.
[2] Scaffidi T., et al. *Phys. Rev. Lett*, 2017, **118**: 226601.

Electron hydrodynamics in 2D confined materials

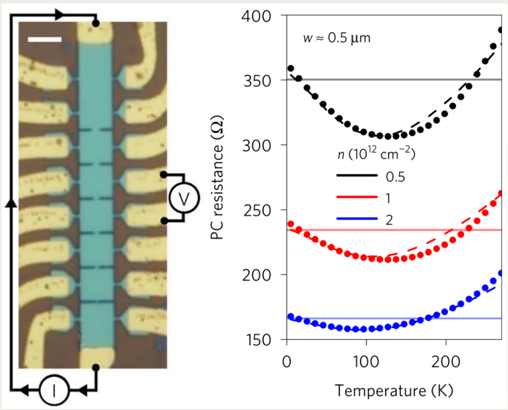

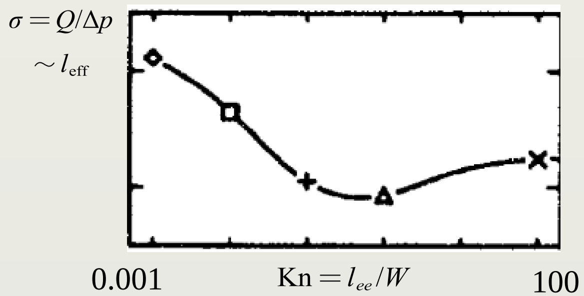

Superballistic flow in confined graphene

(confinement)

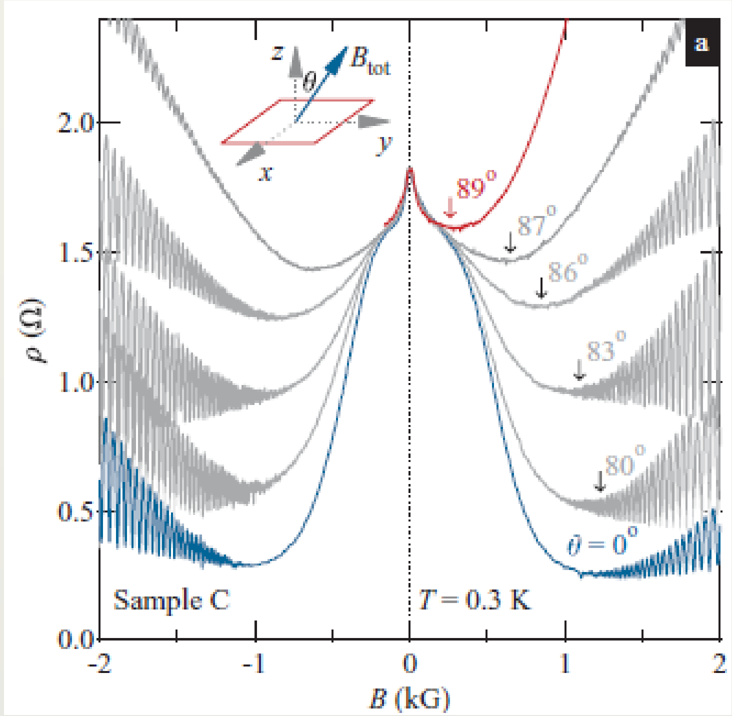

Giant negative magneto-resistance in GaAs/AlGaAs

(magnetic field)

- **How do the magnetic field impact the electric resistance in confined materials?**

[1] Kumar K.R. et al. *Nature Physics*, 2017, **13**(12): 1182-5
[2] Hatke A.T. et al. *Phys. Rev. B*, 2012, **85**: 081304

Magneto-resistance in hydrodynamic regime

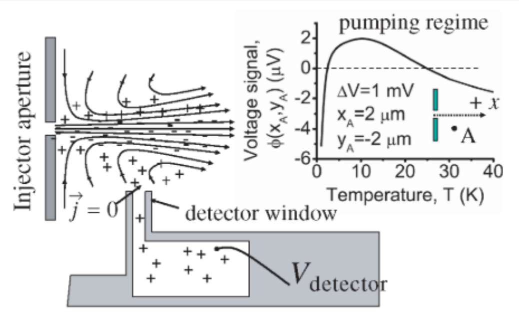

Electron band

- Nature: Single energy band with parabolic spectrum (“simple”)
- Examples: GaAs, GaAs/AlGaAs, $PdCdO_2$, BLG (doped Bi-layer graphene)

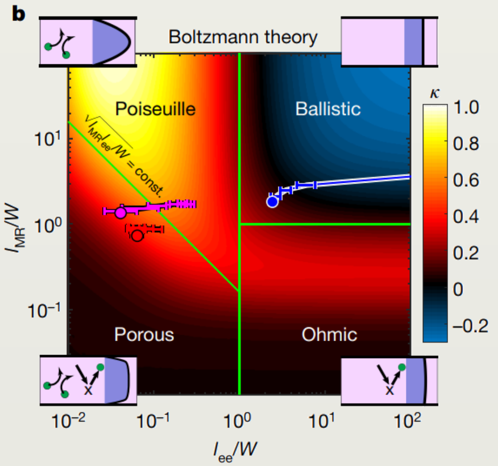

Previous Work

1. Alekseev (2018) presents that **negative magneto-resistance** under small magnetic field in the ballistic transport regime.
2. Holder et al. (2019) find **opposite signs of the curvature of E_y** in the ballistic and hydrodynamic regimes.
3. Mandal et al. (2020) argue that **bulk magneto-resistance** is always positive in the hydrodynamic regime.

Microscopic mechanism can be studied qualitatively, **HOWEVER**,

- quantitative results for problems with various B.C.’s are difficult to obtain;
- it is still unclear about the sign of magneto-resistance in hydrodynamic regime.

[1] Govorov, A.O. and J.J. Heremans, *Physical Review Letters*, **2004**, 92(2): 026803
[2] Alekseev P S and Semina M A *Phys. Rev. Lett*, 2018, **98**: 165412
[3] Chandra M, Kataria G, Sahdev D, et al. *Phys Rev B*, 2019, **99**: 165409.
[4] Mandal I, Lucas A. *Phys Rev B*, 2020, **101**(4): 045122.

Contents

- Introduction to viscous electron transport
- Multiscale modeling and various possibilities
- Case study: Magnetoresistance in hydrodynamic regime
    - Mesoscopic eBTE formulation
    - Verification of numerical methods (DOM)
    - Evaluation of macroscopic description
    - Results of magnetoresistance simulation
- Conclusions

Meso: DOM Algorithm (Formulation)

System Setup: an 2D infinite, conductive and isothermal strip

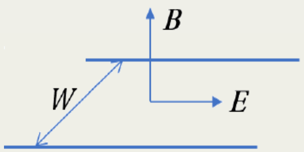

- Displaced Boltzmann equation

$$\frac{\partial \chi}{\partial t} + v_{\mathrm{F}} \boldsymbol{e}_{\rho} \cdot \frac{\partial \chi}{\partial \boldsymbol{r}} + \frac{\boldsymbol{F} \cdot \boldsymbol{e}_{\varphi}}{p_{\mathrm{F}}} \frac{\partial \chi}{\partial \varphi} + e v_{\mathrm{F}} \boldsymbol{E} \cdot \boldsymbol{e}_{\rho} = C_{\delta}(\chi)$$

- Discrete Ordinate Method
  - **simple** and **clear**: directly discretize the BTE
  - **comprehensive**: consider three kinds of scattering
  - **appropriate** to simple geometry (but not easy to generalize)

$$\chi_{\mathrm{ctr}}^{new} = \frac{1}{1 + \alpha_{\mathrm{n}} + \beta_{\mathrm{n}}} \left(-I_{\alpha_{\mathrm{n}}} - I_{\beta_{\mathrm{n}}} - l_{\mathrm{eff}} \boldsymbol{E} \cdot \boldsymbol{e}_{\rho} + I_{\mathrm{scat}} \right).$$

Initialize the displaced distribution function → Calculate the macroscopic quantities and internal ***E*** → Iterate and update the displaced distribution function → Calculate the new macroscopic quantities and their deviation ε to the old ones → $\varepsilon < \varepsilon_0$?

$\varepsilon < \varepsilon_0$? → Calculate the macroscopic quantities and internal ***E***

$\varepsilon < \varepsilon_0$? → Calculate and output the transport properties

Meso: DOM Algorithm (Benchmark)

Electric conductivity

$p = 0$

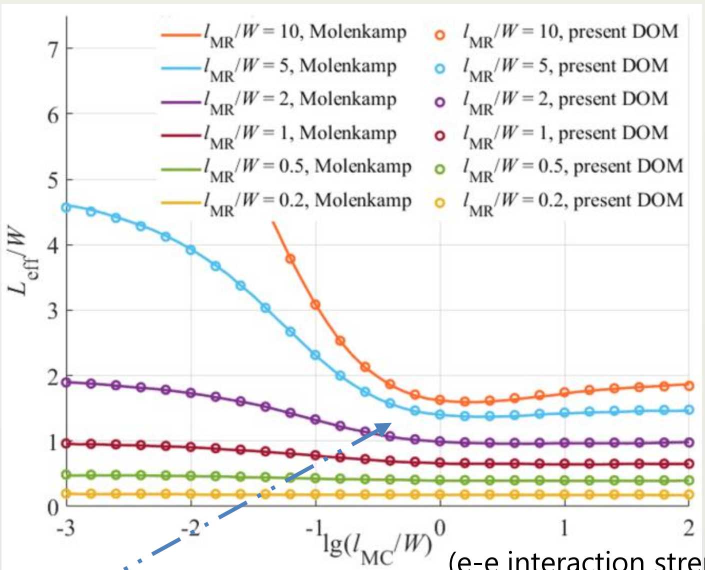

(conductivity)

(e-e interaction strength)

Knudsen-Gurzhi minimum (K-G minimum)

Electron fluid flow profile

$l_{MR}/W = 5.5$, $\alpha = 0.7$

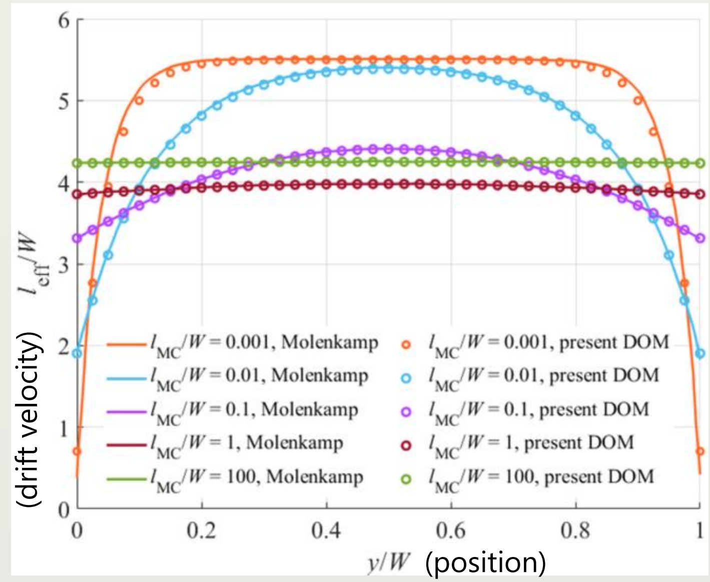

(drift velocity)

(position)

As l_{MC} decreases, parabolic flow recovers.

When $\mathbf{l_{MR}} < \mathbf{l_{MC}}$, the **lattice-electron** interaction dominates: $\sigma \sim v_F l_{MR}$

When $\mathbf{l_{MC}} < \mathbf{l_{MR}}$, the **electron-electron** interaction dominates: $\sigma \sim 1/\eta \sim 1/v_F l_{MC}$

Dots: results from proposed DOM
Lines: results from literature

[1] De Jong M J M, Molenkamp W *Phys. Rev. B*, 1995, **51**: 13389-13402.

Contents

- Introduction to viscous electron transport
- Multiscale modeling and various possibilities
- Case study: Magnetoresistance in hydrodynamic regime
    - Mesoscopic eBTE formulation
    - Verification of numerical methods (DOM)
    - Evaluation of macroscopic description
    - Results of magnetoresistance simulation
- Conclusions

Macro: Grad moment method for up-scaling

- Grad moment method based on Fourier spectra

$$-\mathrm{i}\omega\chi_\omega(\boldsymbol{r},\varphi)+v_\mathrm{F}\boldsymbol{e}_\rho\cdot[\boldsymbol{\nabla}_{\boldsymbol{r}}\chi_\omega(\boldsymbol{r},\varphi)+e\boldsymbol{E}_\omega]+\boxed{(\omega_E+\omega_\mathrm{C})}\nabla_\varphi\chi_\omega(\boldsymbol{r},\varphi)=C_\delta(\chi_\omega).$$

$$\chi_\omega(\boldsymbol{r},\varphi)=:\sum_{n=-\infty}^{+\infty}\chi_{\omega,n}(\boldsymbol{r})e^{\mathrm{i}n\varphi}$$

Electro and magneto cyclotron radius

- Electron hydrodynamic equations (“electron N-S equations”)

$$-\mathrm{i}\omega n_{\delta,\omega}(\boldsymbol{r})+\boldsymbol{\nabla}\cdot\left(\frac{\boldsymbol{P}_\omega}{m^*}\right)=0$$

$$-\mathrm{i}\omega\frac{\boldsymbol{P}_\omega}{m^*}+\boldsymbol{\nabla}\cdot\left(\frac{\boldsymbol{T}_{\delta,\omega}}{m^*}\right)+\frac{v_\mathrm{F}^2D}{2}e\boldsymbol{E}_\omega+\left(\omega_\mathrm{C}\frac{\boldsymbol{P}_\omega}{m^*}+\boldsymbol{\omega}_E\cdot\frac{\boldsymbol{T}_{\delta,\omega}}{p_\mathrm{F}}\right)\times\hat{z}=-\frac{\boldsymbol{P}_\omega/m^*}{\tau_\mathrm{MR}}.$$

Applicable within diffusive regime: $\mathrm{Kn}:=\left(\tilde{l}_\mathrm{MR}{}^{-1}+\tilde{l}_\mathrm{MC}{}^{-1}\right)^{-1}\ll 1$

Macro: Verification of electron N-S equations

$$\nu_{xx}\frac{\mathrm{d}^2u}{\mathrm{d}y^2}+\frac{(-e)}{m^*}E_x-\frac{u}{\tau_{\mathrm{MR}}}=0.$$

$$u|_{y=0}=l_{\mathrm{b}}\frac{\mathrm{d}u}{\mathrm{d}y}\bigg|_{y=0},\quad u|_{y=W}=-l_{\mathrm{b}}\frac{\mathrm{d}u}{\mathrm{d}y}\bigg|_{y=W}$$

$$\Rightarrow$$

$$u=V_0K\left[\lambda+\frac{(e^{\mu\tilde{y}}-1)(e^{\mu(1-\tilde{y})}-1)}{e^{\mu}-1}\right]$$

$$V_0=\frac{(-e)E_x\tau_{\mathrm{MR}}}{m^*},\quad K=\frac{e^{\mu}(1+\lambda)+e^{-\mu}(1-\lambda)-2}{e^{\mu}(1+\lambda)^2-e^{-\mu}(1-\lambda)^2}$$

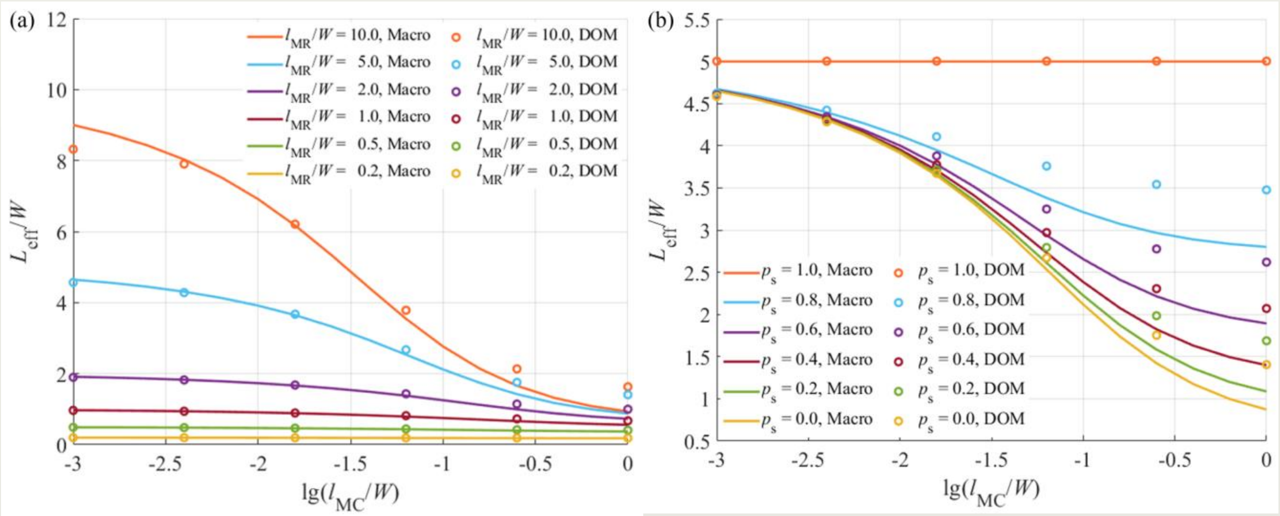

$$\mathrm{Kn}=\left(\tilde{l}_{\mathrm{MR}}{}^{-1}+\tilde{l}_{\mathrm{MC}}{}^{-1}\right)^{-1}\lesssim 0.01$$

Agree well with each other

within **diffusive regime**

(Kn < 0.01, p < 0.6)

DOM results (line) v.s. N-S equation results (dots)

Contents

- Introduction to viscous electron transport
- Multiscale modeling and various possibilities
- Case study: Magnetoresistance in hydrodynamic regime
  - Mesoscopic eBTE formulation
  - Verification of numerical methods (DOM)
  - Evaluation of macroscopic description
  - Results of magnetoresistance simulation
- Conclusions

Result: Magneto-resistance effect (Internal E)

Take the angular term into consideration: how to calculate E_y?

$$\frac{\partial \chi}{\partial t} + v_{\mathrm{F}} \boldsymbol{e}_\rho \cdot \frac{\partial \chi}{\partial \boldsymbol{r}} + \boxed{\frac{\boldsymbol{F} \cdot \boldsymbol{e}_\varphi}{p_{\mathrm{F}}}} \frac{\partial \chi}{\partial \varphi} + e v_{\mathrm{F}} \boldsymbol{E} \cdot \boldsymbol{e}_\rho = C_\delta(\chi) \qquad \boldsymbol{F} = -e(\boldsymbol{E} + \boldsymbol{v} \times \boldsymbol{B})$$

- GCA model for 2D strip with back gate

$$\rho(\boldsymbol{r},t) = en(\boldsymbol{r},t) = CU(\boldsymbol{r},t)$$

chemical electro-static

$$\frac{1}{C} = \frac{1}{C_0} + \frac{1}{C_Q} = \frac{1}{\epsilon_r/4\pi d} + \frac{1}{e^2 \partial n/\partial \mu} \doteq \frac{1}{\epsilon_r/4\pi d}$$

$$E_y(\boldsymbol{r},t) = \nabla_{\boldsymbol{r}} U(\boldsymbol{r},t) = \frac{4\pi e d}{\epsilon_1} \nabla_{\boldsymbol{r}} n(\boldsymbol{r},t)$$

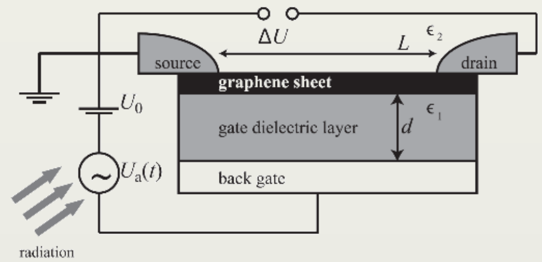

- Self-consistent model for 2D strip without back gate

$$E_y = j_x B - \partial_y n + \frac{1}{2} \partial_y T_{xx}$$

drift screening viscosity

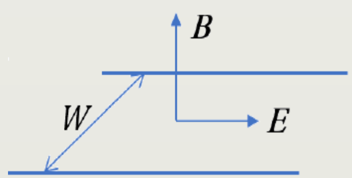

- Poisson equation model for 3D thin film

$$E_y = -\frac{\mathrm{d}\varphi}{\mathrm{d}y}, \quad \frac{\mathrm{d}^2\varphi}{\mathrm{d}y^2} = -\frac{en}{\varepsilon}, \quad E_y|_{\mathrm{bd}} = 0$$

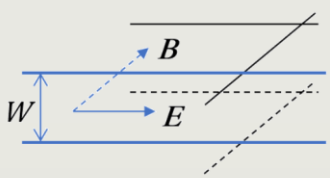

Result: Magneto-resistance effect (Results)

Phase diagram of MR's sign

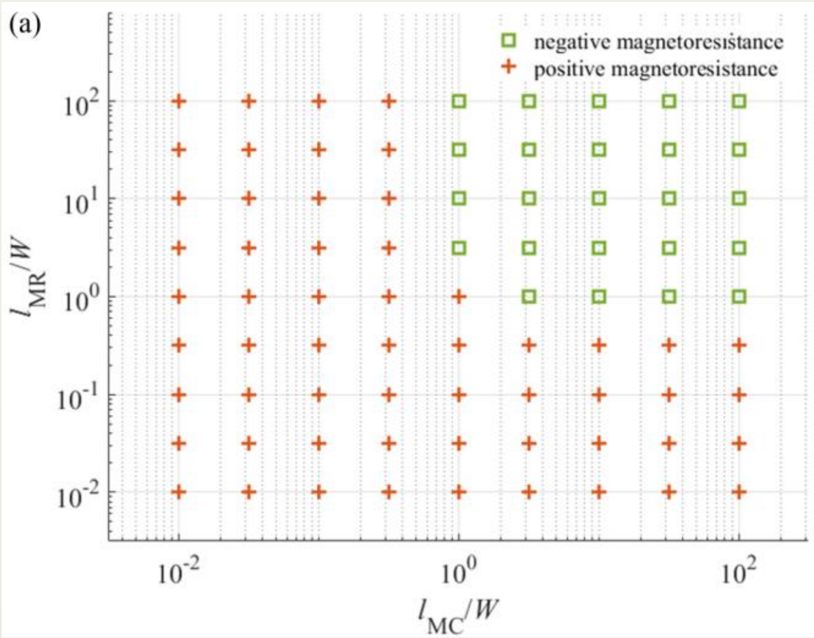

1. Only Poisson equation model gets convergent.
2. Negative MR effect only occurs within the ballistic regime rather than the hydrodynamic regime.
3. Under high electric field, MR effect is always positive.

Exemplars of MR curves under low E

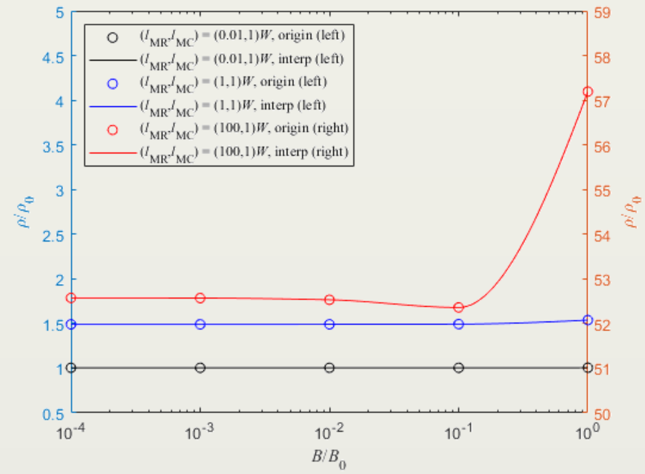

Impact of E's scale on MR curves

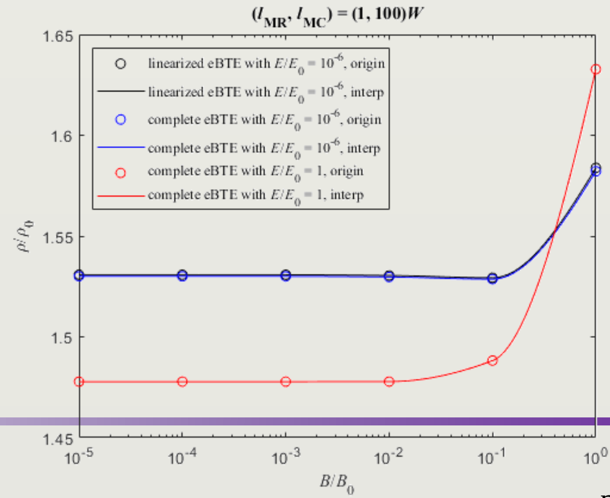

Conclusions

- A numerical algorithm (DOM) based on mesoscopic theory is established, and verified by theoretical solutions successfully. Then the applicability of macroscopic electron N-S equation is clarified, which is valid only within diffusive regime. This **addresses the necessity of utilizing the full formation of Boltzmann equation** instead of linearized displaced eBTE or macroscopic equations while dealing with relevant problems.
- The condition of occurrence of negative magneto-resistance is investigated. **Negative MR effect only occurs within the ballistic regime rather than the hydrodynamic regime under low electric field**. When the electric field becomes large enough compared to the magnetic field, its effect on the deflection of the electrons cannot be neglected and will lead to the positive magneto-resistivity in the whole parameter domain.

Thanks!

Derivation of displaced electron BTE

- Transform the original BTE
  - Expansion of distribution function around equilibrium distribution
  - Split the steep factor $\left(-\frac{\partial f_0}{\partial \varepsilon}\right)$ from displaced distribution function
- Simplification of displaced BTE
  - ignore the high-order effect
  - retain the electric force only
  - ignore the finite temperature effect

$$\frac{\partial f}{\partial t} + \boldsymbol{v}\cdot\frac{\partial f}{\partial \boldsymbol{r}} + \boldsymbol{F}\cdot\frac{\partial f}{\partial \boldsymbol{p}} = C(f)$$

$$\Big\downarrow \; f(\boldsymbol{r},\boldsymbol{p}) =: f_0(\boldsymbol{r},\varepsilon(\boldsymbol{p})) + \delta f(\boldsymbol{r},\boldsymbol{p})$$

$$\frac{\partial \delta f}{\partial t} + \boldsymbol{v}\cdot\frac{\partial \delta f}{\partial \boldsymbol{r}} + \boldsymbol{F}\cdot\frac{\partial \delta f}{\partial \boldsymbol{p}} + S(f_0) = C_\delta(\delta f).$$

$$\Big\downarrow \; S(f_0) \equiv \left(e\mathcal{E} + \frac{\varepsilon-\mu}{T}\nabla_{\boldsymbol{r}}T\right)\cdot\boldsymbol{v}\left(-\frac{\partial f_0}{\partial \varepsilon}\right)$$

$$\frac{\partial \chi}{\partial t} + \boldsymbol{v}\cdot\frac{\partial \chi}{\partial \boldsymbol{r}} + \boldsymbol{F}\cdot\frac{\partial \chi}{\partial \boldsymbol{p}} + S_{\mathcal{E},T} + S_\varepsilon = C_\delta(\chi).$$

$$S_\varepsilon = e\boldsymbol{E}\cdot\boldsymbol{v}\Delta.$$

$$S_{\mathcal{E},T} = \left(e\mathcal{E} + \frac{\varepsilon-\mu}{T}\nabla_{\boldsymbol{r}}T\right)\cdot\boldsymbol{v}$$

$$\boldsymbol{v} =: v_{\mathrm{F}}(\cos\varphi, \sin\varphi)$$

$$\Big\downarrow$$

$$\frac{\partial \chi}{\partial t} + v_{\mathrm{F}}\boldsymbol{e}_\rho\cdot\frac{\partial \chi}{\partial \boldsymbol{r}} + \frac{\boldsymbol{F}\cdot\boldsymbol{e}_\varphi}{p_{\mathrm{F}}}\frac{\partial \chi}{\partial \varphi} + ev_{\mathrm{F}}\boldsymbol{E}\cdot\boldsymbol{e}_\rho = C_\delta(\chi).$$

Essentials of Discrete Ordinate Method

- **Upwind scheme** – Using upwind model points to discretize the derivatives

$$\frac{\partial \chi}{\partial t} + v_{\mathrm{F}} \boldsymbol{e}_{\rho} \cdot \frac{\partial \chi}{\partial \boldsymbol{r}} + \frac{\boldsymbol{F} \cdot \boldsymbol{e}_{\varphi}}{p_{\mathrm{F}}} \frac{\partial \chi}{\partial \varphi} + e v_{\mathrm{F}} \boldsymbol{E} \cdot \boldsymbol{e}_{\rho} = C_{\delta}(\chi).$$

$$\chi_{\mathrm{ctr}}^{new} = \frac{1}{1 + \alpha_{\mathrm{n}} + \beta_{\mathrm{n}}} \left(-I_{\alpha_{\mathrm{n}}} - I_{\beta_{\mathrm{n}}} - l_{\mathrm{eff}} \boldsymbol{E} \cdot \boldsymbol{e}_{\rho} + I_{\mathrm{scat}} \right).$$

- **Gradual Channel Approximation** – Using Q=CU to calculate the internal $\boldsymbol{E}$

$$\boldsymbol{E}_{\mathrm{int}}(\boldsymbol{r}, t) = -\boldsymbol{\nabla}_{\boldsymbol{r}} \phi(\boldsymbol{r}, t) = \boldsymbol{\nabla}_{\boldsymbol{r}} U(\boldsymbol{r}, t) = \frac{4\pi e d_{\epsilon_1}}{\epsilon_1} \boldsymbol{\nabla}_{\boldsymbol{r}} n(\boldsymbol{r}, t) \equiv \frac{4\pi e d_{\epsilon_1}}{\epsilon_1} \boldsymbol{\nabla}_{\boldsymbol{r}} n_{\delta}(\boldsymbol{r}, t).$$

- Statistics of macroscopic quantities

$$n_{\delta}(\boldsymbol{r}, t) := \int \left(f(\boldsymbol{r}, \boldsymbol{p}, t) - f_0(\boldsymbol{r}, \varepsilon(\boldsymbol{p}), t) \right) \frac{2\, \mathrm{d}^2 \boldsymbol{k}}{(2\pi)^2} = D P_0[\chi],$$

$$\boldsymbol{j}(\boldsymbol{r}, t) := \int (-e) \boldsymbol{v} \left(f(\boldsymbol{r}, \boldsymbol{p}, t) - f_0(\boldsymbol{r}, \varepsilon(\boldsymbol{p}), t) \right) \frac{2\, \mathrm{d}^2 \boldsymbol{k}}{(2\pi)^2} = (-e) \frac{D v_{\mathrm{F}}}{2} (P_1[\chi], P_{-1}[\chi])^T.$$

Numerical Scheme of Discrete Ordinate Method

- **Numerical Scheme:** $$\chi_{\mathrm{ctr}}^{new} = \frac{1}{1+\alpha_{\mathrm{n}}+\beta_{\mathrm{n}}}\left(-I_{\alpha_{\mathrm{n}}} - I_{\beta_{\mathrm{n}}} - l_{\mathrm{eff}}\boldsymbol{E}\cdot\boldsymbol{e}_{\rho} + I_{\mathrm{scat}}\right).$$

Parameters

$$\alpha_{\mathrm{n}} := \frac{l_{\mathrm{eff}}\,|\sin\varphi|}{\mathrm{d}y},$$

$$\beta_{\mathrm{n}} := l_{\mathrm{eff}}\,|F_{\mathrm{ext}}|\left(-\frac{\mathrm{sign}(F_{\mathrm{ext}})-1}{2}\frac{1}{\Delta_+} + \frac{\mathrm{sign}(F_{\mathrm{ext}})+1}{2}\frac{1}{\Delta_-}\right)$$

$$I_{\alpha_{\mathrm{n}}} := \alpha_{\mathrm{n}}\left(\frac{\mathrm{sign}(\sin\varphi)-1}{2}\chi_{\mathrm{up}} - \frac{\mathrm{sign}(\sin\varphi)+1}{2}\chi_{\mathrm{down}}\right),$$

$$I_{\beta_{\mathrm{n}}} := \beta_{\mathrm{n}}\left(\frac{\mathrm{sign}(F_{\mathrm{ext}})-1}{2}\chi_{\mathrm{a.w.}} - \frac{\mathrm{sign}(F_{\mathrm{ext}})+1}{2}\chi_{\mathrm{c.w.}}\right),$$

$$I_{\mathrm{scat}} := l_{\mathrm{eff}}\left(\frac{1}{l_{\mathrm{eff}}}P_0[\chi] + \frac{1}{l_{\mathrm{MC}}}P_{\pm 1}[\chi]\right).$$

Notes

a) Discrete velocity space and Gauss quadrature

b) Upwind scheme using virtual time stepping

c) Similar to Lattice Boltzmann Method (LBM)

Strengths

a) Able to capture non-equilibrium effect

b) More freedom to choose parameters